Organic & Biomolecular Chemistry

Cite this: *Org. Biomol. Chem.*, 2012, **10**, 6740

www.rsc.org/obc

PAPER

A highly selective fluorescence sensor for Tin (Sn^{4+}) and its application in imaging live cells†

Qi Wang, Chunyan Li, Ying Zou, Haoxuan Wang, Tao Yi* and Chunhui Huang

Received 10th May 2012, Accepted 21st June 2012
DOI: 10.1039/c2ob25895a

A naphthalimide–rhodamine B derivative was synthesized as a fluorescence turn-ON chemodosimeter for Sn^{4+}. A colour change and marked enhancement of fluorescence was found in the presence of Sn^{4+}, Cu^{2+} and Cr^{3+} due to the ring open reaction of rhodamine and a fluorescence resonance energy transfer process. Addition of the strong chelating agent ethylenediaminetetraacetic acid disodium salt (EDTA) partly released the cation from the complex with Sn^{4+} and restored the yellow fluorescence. In addition, the compound can be used as a fluorescent probe for Sn^{4+} in biological systems and may act as a tool with which to study the physiological functions of tin or pathogenesis in the human body.

Introduction

Tin is an essential trace mineral for humans and is found in the greatest amounts in the adrenal glands, liver, brain, spleen and thyroid gland.[1] A deficiency of tin may result in poor growth and hearing loss and there is some evidence that tin is involved in growth factors and cancer prevention. Some toxic effects of tin have been reported, with symptoms limited mostly to gastrointestinal complaints such as nausea, abdominal pain and vomiting.[1c] However, we have little other knowledge of the role of tin in human metabolism due to the lack of effective tools with which to study the mechanisms.

In recent years, significant emphasis has been placed on the development of new, highly selective fluorescent sensors of metal cations because of their potential applications in biochemistry and environmental research.[2] Many kinds of signaling mechanisms have been proposed and utilized for optical detection of metal ions, including photo-induced electron/energy transfer (PET),[3] intramolecular charge transfer (ICT),[4] fluorescence resonance energy transfer (FRET),[5] and so on. Some of those sensors can also be applied in fluorescence bioimaging,[6] which causes little cell damage and is highly sensitive with high-speed spatial analysis of living cells.[7,8] Specifically, FRET imaging that affords simultaneous recording of two emission intensities at different wavelengths in the presence and absence of analytes has provided a facile method for visualizing complex biological processes at the molecular level.[9] This technique appears to be suited to the study of physiological functions or pathogenesis of tin in the human body. To our knowledge, however, there is no report of a fluorescent probe used as a selective Sn^{4+} sensor.

Rhodamine B is widely used as a fluorescent probe for the detection of cysteine[10] and metal ions,[11] including Cu^{2+},[12] Cr^{3+},[13] Fe^{3+},[14] and Hg^{2+},[15] due to the ring opening reaction of rhodamine. Naphthalimides are classic fluorescent dyes whose electronic absorption and emission depend on the properties of the molecular structure and surrounding medium.[16] Herein, the two fluorochromes are combined into a new fluorescent probe **1** (Scheme 1), in which rhodamine B selectively senses cations with high quantum yields and good photostability,[15b] and naphthalimide can be used as a second fluorescent chemodosimeter for FRET process.[6,11] This naphthalimide–rhodamine B derivative can selectively detect Sn^{4+} from other metal ions by the use of ethylenediaminetetraacetic acid (EDTA) as a second ligand, and thus be used as a Sn^{4+} sensor in living cells.

Experiment

General instruments for characterization

^1H NMR and ^{13}C NMR spectra were recorded on a Varian Mercury Plus 400 spectrometer with tetramethylsilane as the internal standard. The element analysis was performed on a VarioEL III O-Element Analyzer system. Electrospray ionization mass spectra (ESI-MS) were measured on a Micromass LCTTM system. Melting points were determined on a hot-plate melting point apparatus XT4-100A and uncorrected. UV-Vis spectra were recorded on a Shimadzu UV-2250 spectrophotometer. Fluorescence spectra were recorded on an Edinburgh FLS-920 spectrophotometer. All pH measurements were made with a Model PHS-2F meter.

Department of Chemistry, Fudan University, 220 Handan Road, Shanghai, China. E-mail: yitao@fudan.edu.cn; Fax: +86-21-55664621; Tel: +86-21-55664330

†Electronic supplementary information (ESI) available: Details of supplementary spectra and images. See DOI: 10.1039/c2ob25895a

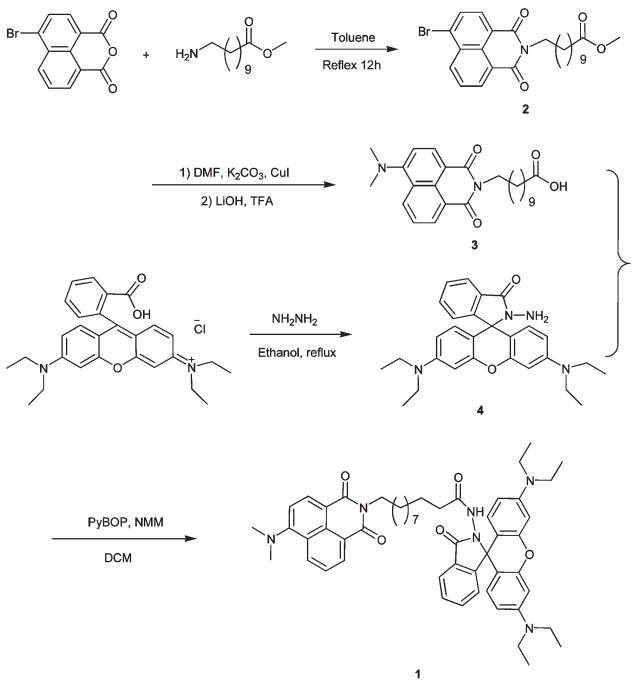

Scheme 1 Chemical structure and synthetic routine of **1**.

Synthesis of the sensor

The synthesis of compound **1** is shown in Scheme 1. Compound **2** has been reported in our previous work[17] and checked by ^{1}H NMR, ^{13}C NMR and ESI-MS. The *N*,*N*-dimethylamino group was bonded to the naphthalic group of **2** using CuI as the catalyst. The methyl ester was cleaved by LiOH to yield **3**.[17] The procedure for the synthesis of rhodamine B hydrazide **4** is described in the literature.[12] Compounds **3** and **4** were coupled using (benzotriazol-1-yloxy)tripyrrolidinophosphonium hexafluorophosphate (PyBOP) in dichloromethane as the coupling reagent to yield compound **1**. The structure of **1** was confirmed by ^{1}H NMR, ^{13}C NMR spectroscopy, and MALDI-TOF mass spectrometry. The details of the synthesis were as follows.

N-(11-Carboxydecyl)-4-dimethylamino-1,8-naphthalimide (3)

To 250 mL flask, compound **2** (0.8 g, 1.7 mmol), K_2CO_3 (0.5 g, 3.6 mmol) and CuI (trace) was dissolved in 50 mL dry DMF. The mixture was refluxed under a nitrogen atmosphere for 12 hours. Then the mixture was cooled and solvent was removed under reduced pressure. The product was purified by column chromatograph using ethyl acetate–petroleum ether (1 : 3, v/v) as an eluent to give a yellow solid (0.55 g, 78%). The obtained product was dissolved in a mixture of 100 mL THF–H_2O (1 : 1, v/v), then LiOH (0.5 g) was added to the solution and stirred at RT for 48 hours. The solvent was evaporated and the white solid was neutralized with HCl (1 M). The product was then extracted with dichloromethane (50 × 3 mL) from the solution. The crude product was purified by flash chromatography using ethyl acetate–petroleum ether (2 : 3, v/v) as an eluent. The product was obtained as a yellow solid, yield 0.53 g, 96%. M.p. 73–75 °C; ^{1}H NMR (400 MHz, $CDCl_3$), δ (ppm) 8.59 (d, 1H, J = 12 Hz), 8.50 (d, 1H, J = 12 Hz), 8.46 (d, 1H, J = 12 Hz), 7.68 (t, 1H, J = 12 Hz), 7.14 (d, 1H, J = 16 Hz), 4.17 (t, 2H, J = 7 Hz), 3.12 (s, 6H), 2.36 (t, 2H, J = 12 Hz), 1.75–1.63 (m, 4H), 1.43 (m, 2H), 1.30 (m, 12H); ^{13}C NMR (100 MHz, $CDCl_3$), δ (ppm) 164.6, 164.1, 132.6, 131.1, 125.3, 1240.9, 123.2, 113.4, 44.8, 40.3, 33.7, 29.4, 29.3, 29.2, 29.0, 28.9, 28.1, 27.0, 24.6. MS (EI) calculated for $C_{25}H_{32}N_2O_4$: 424.24; found: 425.24 $[M + H]^+$. Anal. calcd for $C_{25}H_{32}N_2O_4$: C 70.73, H 7.60, N 6.60; found: C 70.69, H 7.61, N 6.58.

Rhodamine B hydrazide (4)

To a 100 mL flask, rhodamine B (1.8 g, 3.8 mmol) was dissolved in 50 mL ethanol. 3.0 mL (excess) hydrazine hydrate (85%) was then added dropwise with vigorous stirring at room temperature. The mixture was heated to reflux in an oil bath for 2 hours. The solution changed from dark purple to light orange. Then the mixture was cooled and solvent was removed under reduced pressure. HCl (1 M, about 70 mL) was added to the solid to generate a clear red solution. After that, NaOH (1 M, about 70 mL) was added slowly with stirring until the pH of the solution reached 9. The resulting precipitate was filtrated and washed 3 times with 15 mL water. After drying over P_4O_{10} *in vacuo*, rhodamine B hydrazide was obtained as a pink solid (1.4 g, 81%). M.p. 176–177 °C. ^{1}H NMR (400 MHz, $CDCl_3$), δ (ppm) 1.16 (t, 12H, J = 7.0 Hz), 3.32 (q, 8H, J = 7.0 Hz), 3.61 (bs, 2H), 6.28 (q, J = 2.4 Hz), 6.41(d, 2H, J = 2.4 Hz), 6.46 (d, 2H, J = 8.8 Hz), 7.09–7.11 (m, 1H), 7.43–7.45 (m, 1H), 7.92–7-94 (m, 1H,). ^{13}C NMR (100 MHz, $CDCl_3$), δ (ppm): 12.84, 44.59, 66.11, 98.21, 104.83, 108.25, 123.18, 124.04, 128.29, 128.31, 130.26, 132.70, 149.09, 151.78, 154.07, 166.32. ESI mass calculated for $C_{28}H_{32}N_4O_2$: 456.25, found: 456.3. Anal. calcd for $C_{28}H_{32}N_4O_2$: C 73.66, H 7.06, N 12.27; found: C 73.32, H 7.09, N 12.27.

Compound 1

A mixture of **3** (0.3 g, 0.07 mmol, 1 eq), PyBOP (0.35 g, 0.08 mmol, 1.1 eq) and *N*-methylmorpholine (0.6 mL) was stirred in dichloromethane (50 mL) at room temperature for 3 hours. **4** (0.31 g, 0.07 mmol, 1 eq) was added and the resulting solution was stirred overnight. After TLC showed completely disappearance of **3**, the solvent was evaporated and the crude product was further purified by flash chromatography using ethyl acetate–dichloromethane (1 : 3, v/v) as an eluent and yielding a yellow solid (0.31 g, 46%). M.p. 156–159 °C; ^{1}H NMR (400 MHz, $CDCl_3$), δ (ppm) 8.58 (d, 1H, J = 12 Hz), 8.49 (d, 1H, J = 12 Hz), 8.44 (d, 1H, J = 12 Hz), 7.93 (t, 1H, J = 12 Hz), 7.66 (t, 1H, J = 16 Hz), 7.45 (t, 2H, J = 6 Hz), 7.11 (t, 1H, J = 8 Hz), 6.45 (d, 2H, J = 8 Hz), 6.42 (d, 2H, J = 8 Hz), 6.28 (d, 2H, J = 8 Hz), 4.15 (t, 2H, J = 7 Hz), 3.61 (t, 2H), 3.35 (q, 8H, J = 12 Hz), 3.12 (s, 6H), 2.44 (m, 2H), 1.75–1.63 (m, 2H), 1.41–1.27 (m, 12H), 1.17 (m, 12H); ^{13}C NMR (100 MHz, $CDCl_3$), δ (ppm) 166.6, 153.8, 151.6, 148.9, 132.4, 130.9, 130.5, 128.0, 124.9, 123.8, 122.9, 113.3, 108.0, 104.6, 98.0, 67.0, 46.3, 46.2, 44.7, 44.3, 29.4, 29.3, 26.5, 26.4, 26.3, 26.2, 12.6. MALDI-TOF mass calculated for $C_{53}H_{62}ClN_6NaO_5$:

921.53; found: 922.45 $[M + H]^+$. Anal. calcd for $C_{53}H_{62}N_6O_5$: C 73.75, H 7.24, N 9.74; found: C 73.65, H 7.28, N 9.69.

Metal ion sensing procedures

The solutions of the metal ions (2.5 mM) were prepared in deionized water. A stock solution of **1** (1 mM) was prepared in ethanol and was then diluted to 20 μM with ethanol–water (2 : 1, v/v) for spectral measurement. In titration experiments, each time a 2.5 mL solution of **1** (20 μM) was filled in a quartz optical cell of 1 cm optical path length, and the Sn^{4+} stock solution was added into the quartz optical cell gradually by using a micro-pipette. Spectral data were recorded at 5 min after the addition. In selectivity experiments, the test samples were prepared by placing appropriate amounts of metal ion stock into 2.5 mL solution of **1** (20 μM).

For fluorescence measurements, excitation was provided at 420 nm, and emission was collected from 435 to 750 nm. The binding constant was calculated from the emission intensity – titration curve according to the following equation.[18]

$$I_F{}^0/(I_F - I_F{}^0) = [a/(b-a)][(1/K_S[M]) + 1]$$

where $I_F{}^0$ is the emission intensity of **1** at 580 nm, I_F is the emission intensity of **1** at 580 nm upon addition of different amount of Sn(IV). [M] stands for the concentration of Sn(IV); *a* and *b* are constants. The association constant values K_S is given by the ratio intercept/slope.

Cell culture

The HeLa cell line was provided by Institute of Biochemistry and Cell Biology (China). Cells were grown in MEM (Modified Eagle's Medium) supplemented with 10% FBS (Fetal Bovine Serum) and 5% CO_2 at 25 °C. Cells (5×10^8 L^{-1}) were plated on 18 mm glass coverslips and allowed to adhere for 24 hours. Experiments to assess Sn(IV) uptake were performed in the same media supplemented with 50 μM $SnCl_4$ for 30 min.

Fluorescence imaging

Confocal fluorescence imaging was performed with an OLYMPUS IX81 laser scanning microscope and a 60× oil-immersion objective lens. Excitation of **1**-loaded cells at 543 nm was carried out with a semiconductor laser, and emission was collected at 560–600 nm (single channel). The data for ratio fluorescence imaging were analyzed using software package provided by OLYMPUS instruments. Immediately before the experiments, cells were washed with PBS buffer and then incubated with 50 μM **1** in PBS for 30 min at 25 °C. Cell imaging was then carried out after washing cells with PBS.

Results and discussion

Metal ion response

High-level selectivity is of paramount importance for an excellent chemosensor.[19] In the present work, we extended our studies of the selective coordination of cations with **1** by means of fluorescence spectroscopy to include the related heavy, transition and main group metal ions. A solution of **1** (20 μM) in optimized ethanol/4-(2-hydroxyethyl)piperidine-1-ethanesulfonic acid (Hepes) buffer (2 : 1, v/v, pH 7.2) is pale yellow and emits yellow fluorescent light, indicating that the spirocyclic form of rhodamine B is retained (Fig. 1a). The weak absorption band at ~418 nm is ascribed to a 1,8-naphthalimide chromophore (Fig. 2a). The wavelength of the related emission is 523 nm (Fig. 2b). Compound **1** has little variation of absorption or

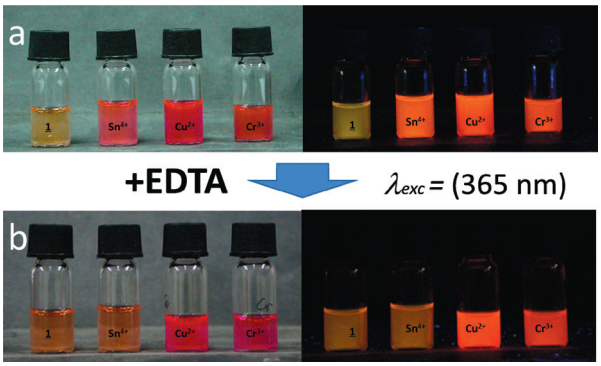

Fig. 1 Change in color and fluorescence of **1** (20 μM) (a) upon addition of Sn^{4+}, Cu^{2+}, Cr^{3+} (200 μM, respectively) and (b) by further addition of EDTA (1 mM) to different solvents.

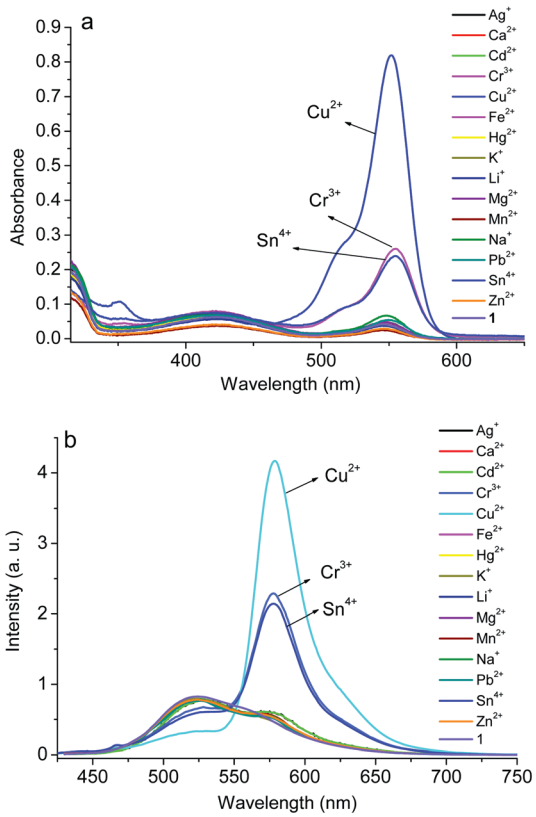

Fig. 2 Absorption (a) and fluorescence emission (b, λ_{ex} = 420 nm) changes of **1** (20 μM) in ethanol–Hepes (2 : 1, v/v, pH 7.2) by addition of 200 μM different metal ions (Ag^+, Ca^{2+}, Cd^{2+}, Cr^{3+}, Cu^{2+}, Fe^{2+}, Hg^{2+}, K^+, Li^+, Mg^{2+}, Mn^{2+}, Na^+, Pb^{2+}, Sn^{4+}, Zn^{2+}).

fluorescence upon the addition of excess metal ions, such as Na^+, K^+, Mg^{2+}, Ca^{2+}, Li^+, Fe^{2+}, Cd^{2+}, Ag^+, Mn^{2+}, Hg^{2+}, Zn^{2+} and Pb^{2+} (see Fig. S1, ESI†). However, within 1 min following the addition of Cu^{2+}, Cr^{3+} and Sn^{4+} there was a marked change of color from light yellow to red with a maximum absorption wavelength of 555 nm (Fig. 1a and 2a). The fluorescent intensity of **1** + *M* (where *M* is Sn^{4+}, Cu^{2+} or Cr^{3+}) was enhanced and the emission color was changed from light yellow (523 nm) to orange (580 nm) (Fig. 2b). However, when EDTA was added to a solution of **1** + *M*, complex **1** + Sn^{4+} was partly restored to its original color with the orange fluorescent fading to yellow within 30 min. The red color and orange fluorescence of **1** + Cu^{2+} and **1** + Cr^{3+} were practically unchanged (Fig. 1b). Thus, this system could be used for the real-time monitoring of Sn^{4+} in cells and organisms *in vivo*.

An optimized ethanol–Hepes buffer (2 : 1, v/v, pH 7.2) solution of **1** (20 μM) was used for titration experiments. The absorbance at 418 nm of solutions of **1** was little changed following addition of Sn^{4+} (0–10 eq); however, a new absorption peak appeared at ~555 nm (Fig. 3a), indicating the formation of the ring open amide form of **1** as a result of cation binding. The detection limit of this chemosensor for Sn^{4+} was estimated to be 1.1×10^{-5} M by absorption spectral change upon addition of Sn^{4+} (see Fig. S2, ESI†).

Moreover, when excited at 420 nm, addition of Sn^{4+} to a solution of **1** caused marked enhancement of the emission band at 580 nm and the intensity of the fluorescent peak at 523 nm gradually decreased. This is due to the FRET process from 1,8-naphthalimide to the open form of rhodamine (Fig. 3b). With the addition of 10 eq Sn^{4+}, the ratio of emission intensity of rhodamine B and 1,8-naphthalimide at 580 nm and 523 nm (F_{580}/F_{523}) varied from 0.72 to 2.46, corresponding to a 3.4-fold enhancement. A non-linear fit of the fluorescence titration curve exhibited a 1 : 1 stoichiometry for Sn^{4+} and **1**, with an association constant $K_a = (4.73 \pm 0.05) \times 10^3$ M^{-1} (see Fig. S3 in ESI†).[20]

The efficiency of the energy transfer (*E*) was investigated according to Förster theory.[21] The results are shown in Fig. 4. Before the addition of Sn^{4+}, the fluorescence lifetime of **1** in solution (2.0×10^{-5} M) demonstrated a single exponential decay with a lifetime of $\tau_D = 4.71$ ns and this emission decay becomes faster with an addition of Sn^{4+} (see Fig. S6 in ESI†). The value of *E* is also enhanced with increasing of Sn^{4+}. For example, with the addition of equivalent of Sn^{4+} increase from 0.25 to 4.0 eq in dilute solution of **1**, the energy transfer efficiency from naphthalimide to rhodamine is increased from 0.4 to 21.6%.

The peak at 555 nm in the absorption spectrum of **1** + Sn^{4+} was decreased dramatically following further addition of 20 eq EDTA (Fig. 3c). The lowering of the emission curve indicated that EDTA had extracted the Sn^{4+} from the complex and partly recovered the naphthalimide fluorescence at 523 nm. This can be explained by the difference between the association constants for EDTA-Sn and **1**-Sn. $K_{EDTA\text{-}Sn}$ (3.16×10^{34} M^{-1})[22] is much larger than $K_{\mathbf{1}\text{-}Sn}$ (4.7×10^3 M^{-1}); therefore, Sn^{4+} acts as a trigger for fluorescence switch-ON and EDTA acts as a trigger for fluorescence switch-OFF. The ratio of the emission intensity of rhodamine B to that of 1,8-naphthalimide at 580 nm and 523 nm (F_{580}/F_{523}) was decreased from 2.43 to 1.3 (Fig. 3d). As compared with Sn^{4+}, the $K_{\mathbf{1}\text{-}M}$ (M = Cr^{3+}, Cu^{2+}) is larger, even

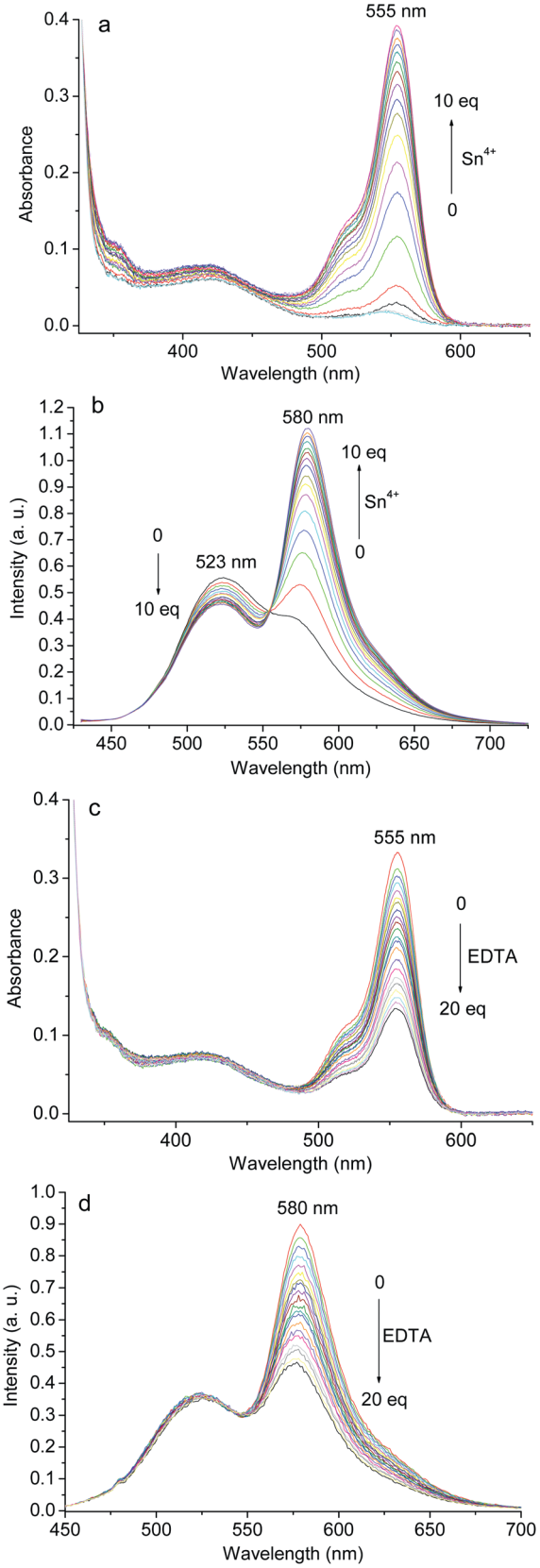

Fig. 3 Absorption (a, c) and fluorescence (b, d) spectra of **1** (20 μM) in ethanol–Hepes (2 : 1, v/v) upon addition of 0–10 eq of Sn^{4+} (a, b), followed by addition of 0–20 eq of EDTA (c, d); measurements were made at 5 min intervals (λ_{ex} = 420 nm).

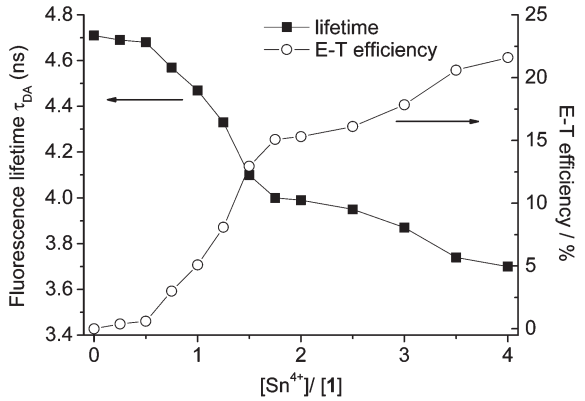

Fig. 4 Fluorescence lifetime and energy transfer (ET) efficiency of **1** on addition of different amounts of Sn^{4+} (0–4.0 eq) in ethanol–Hepes (2 : 1, v/v, pH 7.2) ([**1**] = 2.0×10^{-5} M).

Table 1 Association constants of M (M = Sn^{4+}, Cr^{3+}, Cu^{2+}) with **1** and EDTA

M	Sn^{4+}	Cr^{3+}	Cu^{2+}
$K_{\mathbf{1}\text{-M}}$	$(4.73 \pm 0.05) \times 10^{3}$ [a]	$(2.32 \pm 0.01) \times 10^{4}$ [a]	$(1.94 \pm 0.03) \times 10^{5}$ [a]
$K_{\text{EDTA-M}}$	3.16×10^{34} [b]	2.5×10^{23} [c]	6.3×10^{18} [c]
$K_{\text{EDTA-M}}/K_{\mathbf{1}\text{-M}}$	6.7×10^{30}	1.08×10^{19}	3.3×10^{13}

[a] $K_{\mathbf{1}\text{-M}}$ are calculated with the method in Fig. S3 and S4 in ESI.† [b] Data from ref. 22. [c] Data from ref. 23.

though the difference is not so drastic ($K_{\mathbf{1}\text{-Cr}} = (2.32 \pm 0.01) \times 10^4$; $K_{\mathbf{1}\text{-Cu}} = (1.94 \pm 0.03) \times 10^5$, see Fig. S4 and S5, ESI†). The most important point is that the $K_{\text{EDTA-M}}$ of Sn^{4+} is 10^{12}–10^{16} order larger that of Cr^{3+} and Cu^{2+} due to the higher positive charge (Table 1). Thus, the ratio of $K_{\text{EDTA-M}}/K_{\mathbf{1}\text{-M}}$ (M = Cr^{3+}, Cu^{2+}) is much smaller than $K_{\text{EDTA-Sn}}/K_{\mathbf{1}\text{-Sn}}$. This explained why the reverse processes of Cr^{3+}, Cu^{2+} are difficult than that of Sn^{4+}. Addition of 50 eq EDTA to **1**-Cu and **1**-Cr for 50 min only resulted 9% and 26% of the decrease on the emission intensity of 580 nm (see Fig. S7 and S8, ESI†).

Sensor mechanism

The sensor mechanism is very important for the practical application of this probe. However, our efforts on preparation of single crystal of Sn^{4+} complex of **1** failed. The probable complexation mechanism of **1** with Sn^{4+} was validated by spectral study and ESI-MS. The spectral change underlying Sn^{4+} sensing suggests that the mechanism involves opening the spirolactam ring of rhodamine by Sn^{4+}. The spirocyclic form of rhodamine B, which is colorless and non-fluorescent, becomes colored and strongly fluorescent in the open form by reaction with metal ions. The Sn^{4+}-promoted ring-opening reaction of **1** occurs instantly upon the addition of Sn^{4+} owing to the strong binding of O atoms with high positive charged Sn^{4+}. The chelation of the two carbonyl O atoms in rhodamine B group stabilizes the structure of the metal complex. After Sn^{4+} is removed by the strong chelator EDTA, compound **1** partly recovers its

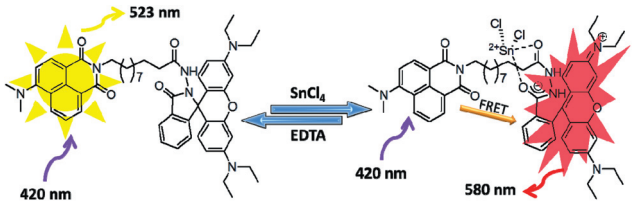

Scheme 2 The Sn^{4+}-sensing mechanism of compound **1**.

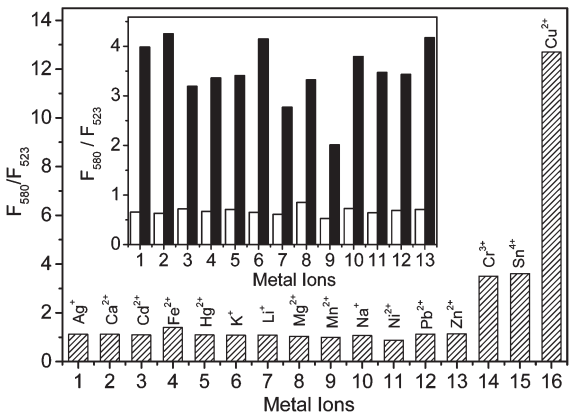

Fig. 5 The ratiometric fluorescence responses (F_{580}/F_{523}) of **1** (20 μM) with various metal ions (*x*-axis) in ethanol–Hepes (2 : 1, v/v). The diagonal bars represent the addition of 200 μM various metal ions to **1**. Inset show competition experiment in which white bars represent the addition of an excess of the appropriate metal ion (2 mM for all cations) to a 20 μM solution of **1**, black bars represent the subsequent addition of 200 μM Sn^{4+} to the solution of 1–13; metal ions: 1, Ag^{+}; 2, Ca^{2+}; 3, Cd^{2+}; 4, Fe^{2+}; 5, Hg^{2+}; 6, K^{+}; 7, Li^{+}; 8, Mg^{2+}; 9, Mn^{2+}; 10, Na^{+}; 11, Ni^{2+}; 12, Pb^{2+}; 13, Zn^{2+}; 14, Cr^{3+}; 15, Sn^{4+}; and 16, Cu^{2+}).

spirolactam ring and exhibits fluorescence emission. This also proves that the sensing mechanism of **1** with Sn^{4+} is a process of complexation.[7a,13]

The proposed binding mode was further verified by the detection of a peak at *m*/*z* 526.3599 (calc. 526.2) corresponding to $[\mathbf{1} + SnCl_2]^{2+}$ by ESI-MS (see Fig. S9, ESI†). Thus, we propose that compound **1** coordinates with Sn^{4+} with 1 : 1 stoichiometry; the two carbonyl O atoms are most likely to be the binding sites for Sn^{4+} on **1** (Scheme 2).

Moreover, the co-existent ions caused negligible interference of Sn^{4+} sensing by **1**, even when other cations were present at micromolar levels (Fig. 5). Fluorescence measurements of **1** in complex with various metal ions revealed excellent selectivity for Sn^{4+}, Cu^{2+} and Cr^{3+}. As shown in Fig. 5, alkali and alkaline-earth metal cations Li^{+}, Na^{+}, K^{+}, Mg^{2+} and Ca^{2+} at a 100-fold excess caused no interference, and transition-metal and heavy-metal ions Zn^{2+}, Fe^{2+}, Mn^{2+}, Ni^{2+}, Cd^{2+}, Hg^{2+}, Ag^{+} and Pb^{2+} gave a weak response. Competition experiments found no obvious change in F_{580}/F_{523} for Sn^{4+} mixed with other metal ions (200 μM), except Cu^{2+} and Cr^{3+}, which can be removed from the complex with **1** by further addition of EDTA (Fig. 5, inset). The pH dependence of **1** indicated that in the acidic environment a proton resulted in the ring open form of the rhodamine B group with increased fluorescent intensity (see

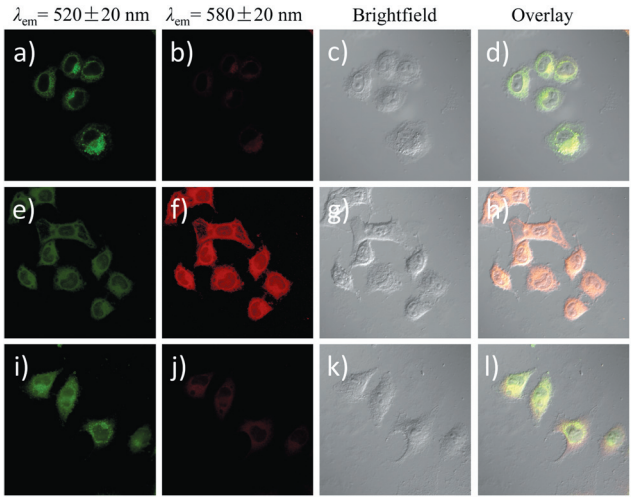

Fig. 6 CLSM images of HeLa cells. (a–d) Cells incubated with 5 μM **1** for 20 min, (e–h) followed with 10 μM Sn^{4+} for 20 min, (i–l) and with 50 μM EDTA for 20 min; emission was collected in green channel at 520 ± 20 nm (a, e and i) and red channel at 580 ± 20 nm (b, f and j); c, g and k are bright field images and d, h and l are overlay images for a, e and i, respectively (λ_{ex} = 405 nm).

Fig. S10, ESI†). However, owing to protonation of the dimethyl amine group on 1,8-naphthalimide, the emission at 523 nm of **1** was increased with decreased pH, resulting in a comparatively small change in F_{580}/F_{523}. This phenomenon is quite different for the reaction of **1** with metal ions. The excellent selectivity of **1** for Sn^{4+} indicates its utility for a wide range of biological applications.

We investigated the applicability of **1** as a Sn^{4+} probe in the fluorescence imaging of living cells as determined by laser scanning confocal microscopy. The fluorescence emissions were collected at both green (520 ± 20 nm) and red channel (580 ± 20 nm) under excitation of 405 nm light. As shown in Fig. 6, HeLa cells incubated with 5 μM **1** for 20 min at 25 °C showed green fluorescence light in green channel and almost no light in red channel (Fig. 6a and b). Upon addition of 10 μM $SnCl_4$ to **1**-loaded HeLa cells, however, the fluorescence intensity of green channel slightly decreased and that of red channel was significantly enhanced (Fig. 6e and f). Bright field measurements after treatment with **1** and $SnCl_4$ confirmed that the cells remained viable throughout the imaging experiments (Fig. 6c and g). Overlay of fluorescence and bright field images revealed that the fluorescence signals were localized in the perinuclear region of the cytosol (Fig. 6d and h), indicating the subcellular distribution of $SnCl_4$ that was internalized within the living cells from the growth medium. Further addition of 50 μM EDTA in the growth medium for 20 min at 25 °C, the fluorescence light of red channel decreased, while the fluorescence intensity of the green channel slightly increased (Fig. 6i and j). The comparison of the overlay images (d, h and l) gave more clear difference among these three states. The results suggest that compound **1** could be used for monitoring intracellular Sn^{4+} in living cells. To the best of our knowledge, this is the first description of a chemodosimeter suitable for monitoring Sn^{4+} in living cells.

Conclusions

In conclusion, we have synthesized a naphthalimide–rhodamine B derivative and demonstrated its utility as a fluorescence switch chemodosimeter that responds stoichiometrically and rapidly to Cu^{2+}, Cr^{3+} and Sn^{4+} in aqueous media. The selective recognition of Sn^{4+} is achieved by addition of EDTA to the solution of **1** + *M* (where *M* is Cu^{2+}, Cr^{3+} or Sn^{4+}), whereby **1** partly recovers its light yellow fluorescence in the complex with Sn^{4+}. The process involves Sn^{4+}-promoted reversible ring opening *via* coordination/disconnection reactions, which we attribute to the lower affinity between Sn^{4+} and the rhodamine moiety. With the help of optical spectra, we can easily identify Sn^{4+} from the other cations. To the best of our knowledge, this is the first example of a fluorescent probe which is sensitive to Sn^{4+}. We anticipate that this new probe will be of great benefit for studying the role of Sn^{4+} in biological systems.

This work was supported by the National Natural Science Foundation of China (91022021, 30890141 and 21125104), the National Basic Research Program of China (2009CB930400), the Program for Innovative Research Team in University (IRT1117), and the Shanghai Leading Academic Discipline Project (B108). Qi Wang thanks for the Department of Macromolecular Science for MALDI-TOF MS experiment.

Notes and references

1 (*a*) Y. Arakawa, *Sangyo Eiseigaku Zasshi*, 1997, **39**, 1–20; (*b*) N. Cardarelli, *Thymus*, 1990, **15**, 223–231; (*c*) L. R. Sherman, J. Masters, R. Peterson and S. Levine, *J. Anal. Toxicol.*, 1986, **10**, 6–9.
2 L. A. Huang, F. J. Chen, P. X. Xi, G. Q. Xie, Z. P. Li, Y. J. Shi, M. Xu, H. Y. Liu, Z. R. Ma, D. C. Bai and Z. Z. Zeng, *Dyes Pigm.*, 2011, **90**, 265–268; A. Helal, M. Rashid, C. H. Choi and H. S. Kim, *Tetrahedron*, 2011, **67**, 2794–2802; S. Goswami, D. Sen and N. K. Das, *Org. Lett.*, 2010, **12**, 856–859; C. H. Zong, K. L. Ai, G. Zhang, H. W. Li and L. H. Lu, *Anal. Chem.*, 2011, **83**, 3126–3132.
3 E. Ballesteros, D. Moreno, T. Gomez, T. Rodriguez, J. Rojo, M. Garcia-Valverde and T. Torroba, *Org. Lett.*, 2009, **11**, 1269–1272; Z. Zhou, N. Li and A. Tong, *Anal. Chim. Acta*, 2011, **702**, 81–86; H. Lu, L. Xiong, H. Liu, M. Yu, Z. Shen, F. Li and X. You, *Org. Biomol. Chem.*, 2009, **7**, 2554–2558.
4 Z. Guo, W. Chen and X. Duan, *Org. Lett.*, 2010, **12**, 2202–2205.
5 B. N. G. Giepmans, S. R. Adams, M. H. Ellisman and R. Y. Tsien, *Science*, 2006, **312**, 217–224; R. H. Newman, M. D. Fosbrink and J. Zhang, *Chem. Rev.*, 2011, **111**, 3614–3666; M. Mank, D. F. Reiff, N. Heim, M. W. Friedrich, A. Borst and O. Griesbeck, *Biophys. J.*, 2006, **90**, 1790–1796; M. J. Ruedas-Rama, X. J. Wang and E. A. H. Hall, *Chem. Commun.*, 2007, 1544–1546.
6 X. Lu, W. Zhu, Y. Xie, X. Gao, F. Li and H. Tian, *Chem.–Eur. J.*, 2010, **16**, 8355–8364; F. Han, Y. Bao, Z. Yang, T. M. Fyles, J. Zhao, X. Peng, J. Fan, Y. Wu and S. Sun, *Chem.–Eur. J.*, 2007, **13**, 2880–2892; L. Deng, W. Wu, H. Guo, J. Zhao, S. Ji, X. Zhang, X. Yuan and C. Zhang, *J. Org. Chem.*, 2011, **76**, 9294–9304; Y. Liu, H. Guo and J. Zhao, *Chem. Commun.*, 2011, **47**, 11471–11473; X. Piao, Y. Zhou, J. Wu, C. Li and T. Yi, *Org. Lett.*, 2009, **11**, 3818–3821.
7 (*a*) K. Huang, H. Yang, Z. Zhou, M. Yu, F. Li, X. Gao, T. Yi and C. Huang, *Org. Lett.*, 2008, **10**, 2557–2560; (*b*) D. J. Stephens and V. J. Allan, *Science*, 2003, **300**, 82–86; (*c*) J. W. Lichtman and J. A. Conchello, *Nat. Methods*, 2005, **2**, 910–919; (*d*) X. Peng, J. Du, J. Fan, Y. Wu, J. Wang, J. Zhao and T. Xu, *J. Am. Chem. Soc.*, 2007, **129**, 1500–1501.
8 M. H. Lim and S. J. Lippard, *Acc. Chem. Res.*, 2007, **40**, 41–51; M. Zhang, M. Yu, F. Li, M. Zhu, M. Li, Y. Gao, L. Li, Z. Liu, J. Zhang, D. Zhang, T. Yi and C. Huang, *J. Am. Chem. Soc.*, 2007, **129**, 10322–10323.
9 H. Ma, E. A. Gibson, P. J. Dittmer, R. Jimenez and A. E. Palmer, *J. Am. Chem. Soc.*, 2012, **134**, 2488–2491; E. A. Jaris-Erijman and T. M. Jovin,

Nat. Biotechnol., 2003, **21**, 1387–1395; E. A. Jaris-Erijman and T. M. Jovin, *Curr. Opin. Chem. Biol.*, 2006, **10**, 409–416, and references therein.
10 H. Li, J. Fan, J. Wang, M. Tian, J. Du, S. Sun, P. Sun and X. Peng, *Chem. Commun.*, 2009, 5904–5906.
11 D. T. Quang and J. S. Kim, *Chem. Rev.*, 2010, **110**, 6280–6301; H. N. Kim, M. H. Lee, H. J. Kim, J. S. Kim and J. Yoon, *Chem. Soc. Rev.*, 2008, **37**, 1465–1472; J. F. Zhang, Y. Zhou, J. Y. Yoon, Y. Kim, S. J. Kim and J. S. Kim, *Org. Lett.*, 2010, **12**, 3852–3855; M. H. Lee, J.-S. Wu, J. W. Lee, J. H. Jung and J. S. Kim, *Org. Lett.*, 2007, **9**, 2501–2504.
12 M. Yu, M. Shi, Z. Chen, F. Li, X. Li, Y. Gao, J. Xu, H. Yang, Z. Zhou, T. Yi and C. Huang, *Chem.–Eur. J.*, 2008, **14**, 6892–6900.
13 Z. Zhou, M. Yu, H. Yang, K. Huang, F. Li, T. Yi and C. Huang, *Chem. Commun.*, 2008, 3387–3389.
14 M. Zhang, Y. Gao, M. Li, M. Yu, F. Li, L. Li, M. Zhu, J. Zhang, T. Yi and C. Huang, *Tetrahedron Lett.*, 2007, **48**, 3709–3712.
15 (*a*) S.-K. Ko, Y.-K. Yang, J. S. Tae and I. J. Shin, *J. Am. Chem. Soc.*, 2006, **128**, 14150–14155; (*b*) H. Yang, Z. Zhou, K. Huang, M. Yu, F. Li, T. Yi and C. Huang, *Org. Lett.*, 2007, **9**, 4729–4732.
16 B. Liu and H. Tian, *J. Mater. Chem.*, 2005, **15**, 2681–2686; B. Liu and H. Tian, *Chem. Commun.*, 2005, 3156–3158.
17 T. Shu, J. Wu, M. Lu, L. Chen, T. Yi, F. Li and C. Huang, *J. Mater. Chem.*, 2008, **18**, 886–893.
18 S. Fery-Forgues, M. T. Le Bris, J. P. Guetté and B. Valeur, *J. Phys. Chem.*, 1988, **92**, 6233–6237.
19 Y. Qu, J. Hua and H. Tian, *Org. Lett.*, 2010, **12**, 3320–3323; Y. Li, L. F. Cao and H. Tian, *J. Org. Chem.*, 2006, **71**, 8279–8282.
20 B. Tang, Y. Xing, P. Li, N. Zhang, F. Yu and G. Yang, *J. Am. Chem. Soc.*, 2007, **129**, 11666–11667; S. Kenmoku, Y. Urano, H. Kojima and T. Nagano, *J. Am. Chem. Soc.*, 2007, **129**, 7313–7318.
21 D. Seth, A. Chakraborty, P. Setua, D. Chakrabarty and N. Sarkar, *J. Phys. Chem. B*, 2005, **109**, 12080–12085; E. Dolghih, A. E. Roitberg and J. L. Krause, *J. Photochem. Photobiol., A*, 2007, **190**, 321–327.
22 J. Kragten, *Talanta*, 1975, **22**, 505–510.
23 P. F. Bell, R. L. Chaney and J. S. Angle, *Plant Soil*, 1991, **130**, 51–62.

